ACS APPLIED MATERIALS & INTERFACES

www.acsami.org

Research Article

Enhancement of Signal-to-Noise Ratio for Serotonin Detection with Well-Designed Nanofilter-Coated Potentiometric Electrochemical Biosensor

Shoichi Nishitani and Toshiya Sakata*

Cite This: *ACS Appl. Mater. Interfaces* 2020, 12, 14761−14769

Read Online

ACCESS | Metrics & More | Article Recommendations | Supporting Information

ABSTRACT: In this paper, we proposed to enhance a signal-to-noise (S/N) ratio for detecting a primary stress marker, serotonin, using a potentiometric biosensor modified by a well-designed nanofilter film. An extended-Au-gate field-effect transistor (EG-Au-gate FET) biosensor exhibits highly sensitive electrochemical detection toward various small biomolecules, including serotonin. Therefore, to enhance the S/N ratio for the serotonin detection, we designed an appropriate nanofilter film on the Au electrode by combining the aryldiazonium salt reduction strategy and boronate affinity. That is, only serotonin can approach the Au sensing surface to generate an electrical signal; interfering biomolecules are prevented from penetrating through the nanofilter, either because large interfering biomolecules cannot permeate through the highly dense, nanoporous multilayer film, or because phenylboronic acids included in the nanofilter captures small interfering biomolecules (e.g., catecholamines). The potentiometric biosensor modified by such a nanofilter film detected serotonin in a model sample solution containing catecholamines, cortisol, and human serum albumin with a high S/N ratio for the serotonin levels in the blood. Furthermore, we found that the effect of the nanofilter directly reflects the binding affinity of the receptors such as phenylboronic acids included in the nanofilter; thus, the selectivity and dynamic range of small target biomolecules can be tuned freely by designing the appropriate receptors for the nanofilter. The results show that a well-designed nanofilter biointerface can be a versatile biosensing platform for point-of-care testing, particularly for a simple stress check.

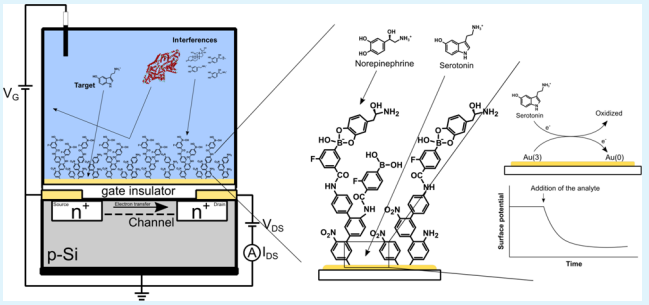

KEYWORDS: *field-effect transistor (FET), nanofilter biointerface, Au electrode, serotonin, signal-to-noise (S/N) ratio*

INTRODUCTION

Recent studies have shown that psychological stress may not only depress people's mood in daily life but also increase the risk of developing severe mental and physical health issues such as depression[1,2] and cancer.[3] In daily life, we can often recognize stress on our own but cannot quantify the amount of exposure to stress because it is a cognitive phenomenon, which makes it difficult to decide the seriousness of the condition. On the other hand, recent progress in biomedical science has identified an increasing number of biomolecules that can be markers of stress exposure. Therefore, the development of biosensors that can quantitatively measure stress markers in our bodily fluids, such as blood, urine, saliva, sweat, and tears, will have a significant impact on the field of medical diagnosis.

The release of neurotransmitters by the nervous system[4,5] and hormones by the endocrine system[6] is one of the essential reactions of our body to stress exposure. Therefore, the primary stress markers include small-biomolecule neurotransmitters and hormones. For example, the expression of the small-biomolecule neurotransmitter serotonin (Figure 1A) correlates with mood regulation and is a promising biomarker for depression.[7] Furthermore, blood serotonin levels correlate to some extent with the development of neuroendocrine tumors.[8] Because serotonin, as well as other neurotransmitters, such as dopamine, norepinephrine (NE), and epinephrine (EP), is produced by oxidative metabolism, electrochemical methods, which enable the detection of redox reactions, it has been widely used to develop biosensors for the detection of small-biomolecule stress markers. In fact, the serotonergic responses to stress in humans were discussed in previous studies.[9,10] For instance, serotonin, dopamine, or simultaneous dopamine and serotonin biosensors were developed using electrochemical methodologies.[11−14] Electrochemical methods are advantageous over other methods such as colorimetric or fluorescence assay because electrochemical detection does not require any extra labeling and can operate in a real-time

Received: October 25, 2019
Accepted: March 5, 2020
Published: March 5, 2020

https://dx.doi.org/10.1021/acsami.9b19309
ACS Appl. Mater. Interfaces 2020, 12, 14761−14769

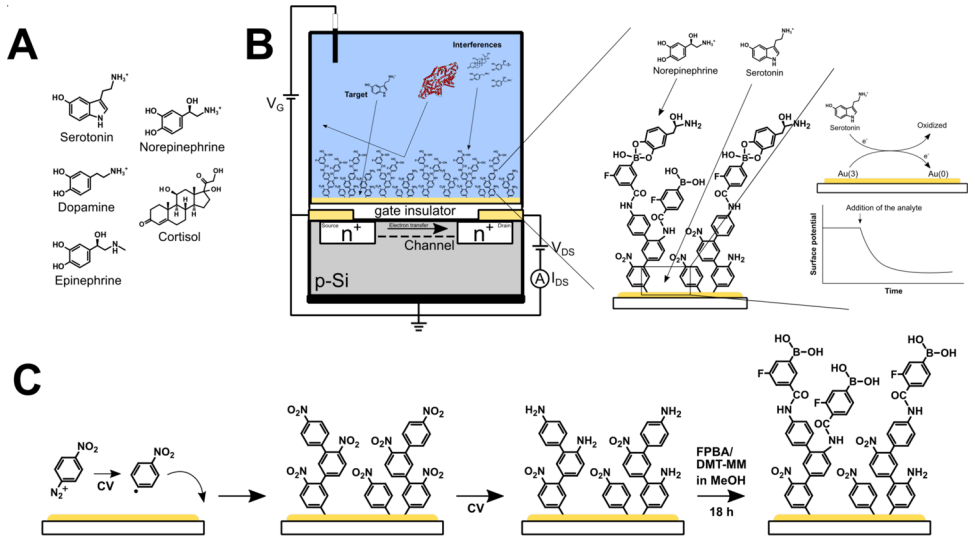

Figure 1. (A) Molecular structures of small-biomolecule stress biomarkers, namely, serotonin, norepinephrine, dopamine, epinephrine, and cortisol. (B) Schematic of the nanofilter-modified extended-Au-gate field-effect transistor (EG-Au-gate FET) biosensor. (C) Development of the nanofilter interface on the Au substrate.

manner.[15] Moreover, the sensor can be miniaturized to develop easy-to-use and low cost, point-of-use devices.[16] However, it is often difficult for electrochemical methods to achieve high selectivity to the target biomolecule, particularly in the case of small-biomolecule stress markers, because the oxidation potentials of the target small biomolecules are very similar, and it is often difficult to differentiate their electrical signals.[17]

In this regard, we have recently proposed a field-effect transistor (FET) biosensor with a polymeric nanofilter biointerface for quantitative small-biomolecule recognition with a high signal-to-noise (S/N) ratio.[18] Solution-gate FETs have been receiving increasing attention in the field of potentiometric biosensor technology owing to their high sensitivity toward changes in gate electrode/electrolyte interfacial potential.[16,19,20] We have also shown that extended-Au-gate FETs (EG-Au-FETs) exhibit potentially high detection sensitivity toward various electrochemically active small biomolecules; the Au surface potential changes with the catalytic electrochemical oxidation of the biomolecules owing to the highly electromotive Au surface (Figure 1B, right).[21,22] Therefore, we designed and developed the polymeric nanofilter biointerface directly on the Au sensing surface to enhance the filtering effect, where the interfering biomolecules are prevented from approaching the Au sensing surface, and only the target small biomolecules can approach and react with the Au sensing surface, generating an electrical signal with a high S/N ratio. As a result, the polymeric nanofilter-coated FET sensor successfully differentiated the electrical signals of two small biomolecules, L-3,4-dihydroxyphenylalanine (L-DOPA) and L-cysteine.[18]

In this study, we designed and developed a nanofilter biointerface for improving the S/N ratio of the serotonin detection. We demonstrated that the use of a multilayer nanofilter film grafted via aryldiazonium salt chemistry could specifically suppress the nonspecific electrical signal generated by the adhesion of large biomolecules to the Au surface. Moreover, the S/N ratio for the detection of serotonin was enhanced by including phenylboronic acid (PBA) in the nanofilter as a receptor to capture interfering small-biomolecule stress markers. Using the nanofilter-modified EG-Au-FET, we demonstrated the quantitative determination of serotonin with a high S/N ratio in the concentration level of blood serotonin in a model sample solution containing similarly structured catecholamines, cortisol, and human serum albumin (HSA). The result was characterized by adhesion isotherm analysis, which showed that the strategy could be widely applied to the detection of various small-biomolecule biomarkers.

RESULTS AND DISCUSSION

In the EG-FET sensor used in this study, the change in the potential at the extended-gate electrode/electrolyte solution interface, which is induced by electrochemical reactions such as equilibrium reactions or nonspecific adsorptions accompanied by changes in molecular charges and redox reactions, causes the change in the conductance of the semiconductor layer on the basis of the field effect. When the extended-gate electrode surface is covered by insulative oxide films (e.g., SiO_2, Ta_2O_5) with hydroxy groups at the surface, the change in the interfacial potential between an electrolyte solution and an oxide film surface resulted from the change in ionic charges based on the equilibrium reaction between hydroxy groups and hydrogen ions. On the other hand, when a catalytically active electrode such as a Au film is used as the extended-gate electrode, redox reactions may occur, which cause the change in the surface potential. In this case, measurement using the EG-FET sensor works similarly to potentiometric, open-circuit potential (OCP) measurement in the electrochemical setup as no current flows through the circuit. In this study, the electrochemical oxidation of serotonin on the Au electrode causes a change in the surface potential, that is, the sensing mechanism is based on the detection of the electrochemical reaction at the Au gate electrode, which is output as the change in the surface potential by the FET. Moreover, measurement using the FET is advantageous over OCP measurement using an electrochemical cell because in the former case, transistors can be miniaturized and arrayed to realize multitarget biosensing in the future, the readout of which can amplify the change in the OCP.

https://dx.doi.org/10.1021/acsami.9b19309
ACS Appl. Mater. Interfaces 2020, 12, 14761−14769

To differentiate serotonin from the other interfering stress biomarkers, we designed the nanofilter biointerface using the following strategies. First, large interfering biomolecules, such as proteins, are prevented from approaching and adhering to the Au sensing surface, thus suppressing nonspecific electrical signals. Therefore, the nanofilter was designed to have a nanoporous structure with a sufficiently high density to prevent large biomolecules from penetrating but at the same time having sufficient spaces for small biomolecules to freely approach the Au sensing surface. Second, the nanofilter captures the interfering small biomolecules before they approach the Au sensing surface, and only the target biomolecule, serotonin, can approach the Au sensing surface, which then electrochemically reacts with the highly active Au electrode, generating the specific change in the surface potential of the Au electrode (Figure 1B).

In this regard, the aryldiazonium salt reduction strategy and boronate affinity were combined to design the nanofilter biointerface. Aryldiazonium salt chemistry is a universal method for surface functionalization on various materials, where the reduction of the aryldiazonium salt produces the corresponding phenyl radicals, leading to the formation of a robust, covalently bound multilayer film through continuous radical reactions.[23,24] In contrast to monolayer films (e.g., self-assembled monolayers), multilayer films will not fully occupy the substrate surface because of steric hindrance, despite their high density, and so only small biomolecules can access the Au surface by penetrating through the narrow spaces between the building block molecules of the multilayer films. The EG-Au-FET biosensor modified by the multilayer film based on the aryldiazonium salt, which was a hydroxyl group at the para-substituent of the benzene ring, suppressed the nonspecific electrical signal generated by the adhesion of proteins to the Au electrode.[18] In this study, a nitrobenzene multilayer was chosen to functionalize the Au surface owing to its commercial availability, ease of use, and wide applicability to further surface functionalization by reducing the nitrophenyl group to the aminophenyl group. Practically, the formation of the nitrophenyl multilayer film and the reduction to the aminophenyl group can be both carried out with a simple electrochemical setup (Figure 1C). Boronate affinity has been extensively used to recognize various biomolecules such as catecholamines[25,26] and saccharides[27−29] owing to its ability to induce pH-triggered reversible binding with cis-diol structures. In this study, the use of boronate affinity introduces the filtering effect to the nanofilter to prevent interfering small biomolecules (i.e., dopamine, norepinephrine, and epinephrine) from penetrating through the nanofilter membrane. That is, the nanofilter can recognize the structural differences between serotonin and catecholamines, where the former has a single hydroxyl group and the latter has two hydroxyl groups on the benzene ring (Figure 1A). Therefore, the interfering small-biomolecule stress biomarkers, mainly the three catecholamines, bind phenylboronic acid (PBA) in the nanofilter before approaching the Au sensing surface, thus suppressing the nonspecific electrical signal, leading to the enhancement of S/N ratios for serotonin recognition. Since the EG-Au-FET is sensitive to biomolecules with high electrochemical activity, the addition of cortisol is expected to have a negligible effect on the sensor response, in contrast to the addition of catecholamines.

The electrochemical grafting of the nitrobenzene multilayer was confirmed by the two distinct reductive current peaks on the cyclic voltammogram (see Figure S1A in the Supporting Information). The density of the grafted multilayer film was calculated from the reduction of the nitrophenyl group to the aminophenyl group in the multilayer film using the relationship derived in the Supporting Information. The grafted film had a density of 12.7 molecules/nm^2 and a thickness of 7 nm, as characterized by atomic force microscopy (AFM) (see Figure S2 in the Supporting Information), indicating the formation of the multilayer film.[30,31] The changes in surface morphology also indicated the successful formation of the porous film, where the modified Au electrodes had a higher roughness than the unmodified Au electrode. Figure S3 (see the Supporting Information) shows the changes the in surface potential induced by the addition of a small biomolecule, ascorbic acid (MW: 176) and large biomolecules, namely, bovine serum albumin (MW: 66 kDa), HSA (MW: 66 kDa), and α-amylase (MW: 62 kDa) in undiluted phosphate-buffered saline (PBS). Accordingly, the aminophenyl multilayer film grafted on the Au electrode had little effect on the sensitivity to the small biomolecule (ascorbic acid), whereas the sensitivity to the macromolecules (bovine serum albumin, HSA, and amylase) was suppressed by nearly 80% compared with that in the case of the unmodified Au electrode. Therefore, the suppression was specific to the addition of large biomolecules. Moreover, the sensor was able to quantitatively determine ascorbic acid in the solution containing HSA with comparable sensitivity. In a previous study, we showed that the use of a nitrobenzene monolayer film leads to almost complete suppression even of the penetration of small biomolecules.[30] Therefore, the use of a multilayer was necessary for a well-balanced inhibitory effect. Determining the spaces in the nanoporous membrane gives the insight to explain the phenomena. According to a previous study, 60% of the nitrophenyl groups are electrochemically active in the multilayer film. Besides, the density and thickness of the fully covered nitrophenyl monolayer on the Au electrode were 6.2×10^{-10} mol/cm^2 and 0.8 nm, respectively.[31,32] Therefore, the fully covered nitrophenyl monolayer film formed by the reduction of the aryldiazonium salt had a density of 3.7 molecules/nm^2. On the other hand, the grafting density of the multilayer film per layer in this study was 2.4 molecules/nm^2, assuming that each layer had the same density. Therefore, the multilayer film had extra spaces for about 1.3 molecules/nm^2 in each layer compared with the monolayer film with the maximum coverage, which is only sufficient for small biomolecules to penetrate through the film and access the Au electrode.

In the next step, the aminophenyl multilayer film on the Au electrode was further functionalized by PBA to complete the nanofilter fabrication for serotonin recognition with a high S/N ratio. Here, the PBA functional group was covalently bound to the multilayer film by merely immersing the aminophenyl-functionalized Au substrate in the solution containing PBA and the catalyst. As a control group, a sensor without PBA functionalization was prepared by also immersing the substrate in the same solution containing PBA but before the electrochemical reduction of the nitrophenyl group to the aminophenyl group (i.e., amidation did not occur). Then, the multilayer film of the control group was subjected to cyclic voltammetry (CV) after immersing it in the PBA solution to control the electrochemical activity of the Au surface. The cyclic voltammetry confirmed that the nitrophenyl group on the control substrate remained electrochemically active (see Figure S4 in the Supporting Information). Furthermore, the cyclic voltammogram after ten potential cycles was identical to

https://dx.doi.org/10.1021/acsami.9b19309
ACS Appl. Mater. Interfaces 2020, 12, 14761−14769

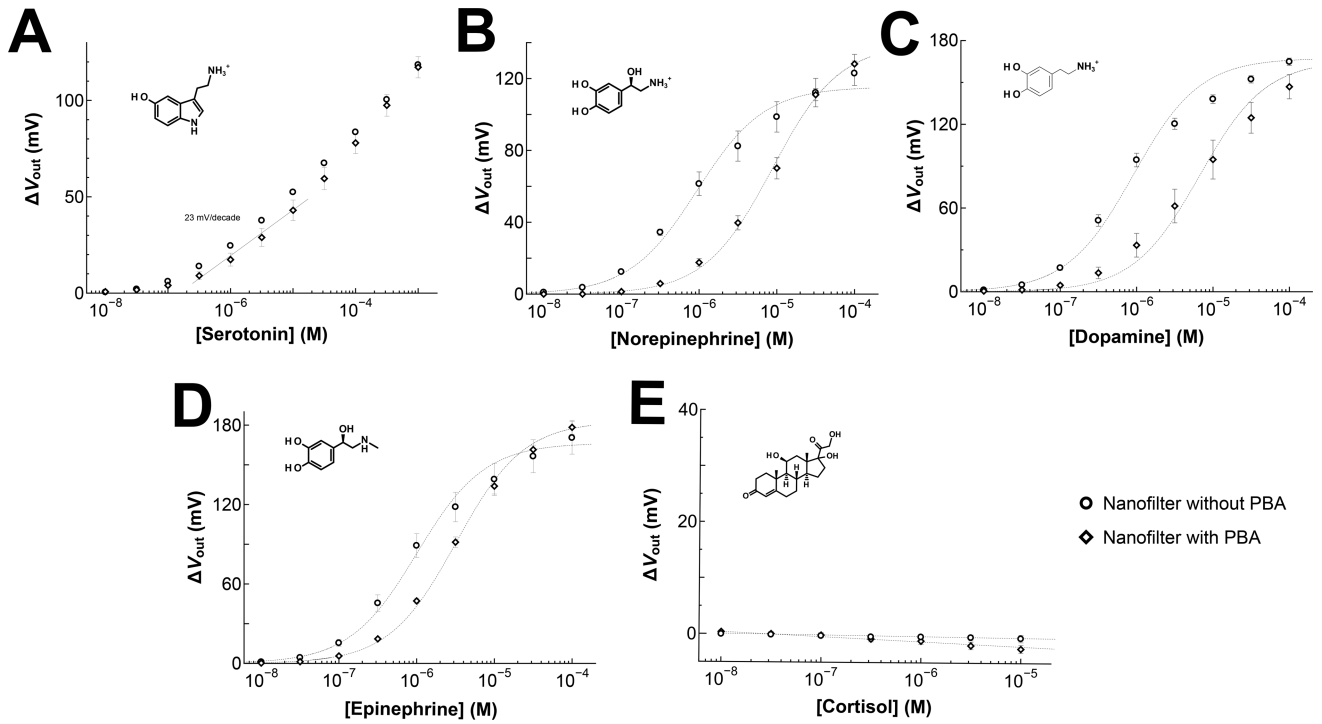

Figure 2. Changes in the surface potential of the sensors modified by nanofilters with (diamonds) and without (circles) PBA vs the analyte concentration on a logarithmic scale. (A) Serotonin (N = 2), (B) norepinephrine (N = 4), (C) dopamine (N = 4), (D) epinephrine (N = 6), and (E) cortisol. Error bars represent the standard error determined from the number of experiments shown for each analyte. The experiments were performed for each analyte using different electrodes with the number of experiments shown. The calibration curve is based on the Langmuir isotherm equation, as described in the Supporting Information.

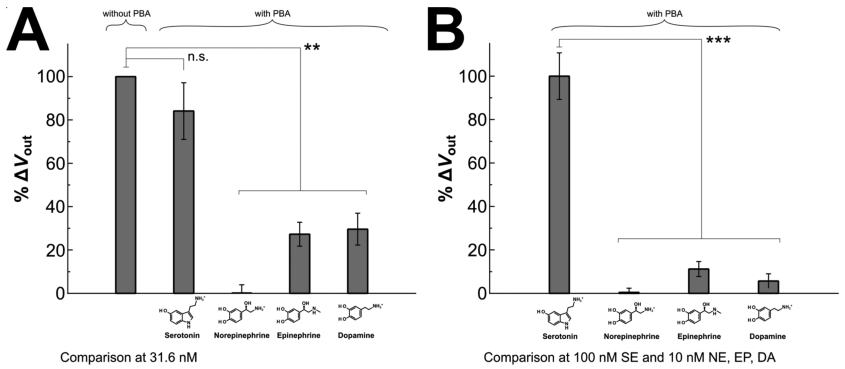

Figure 3. (A) Percent suppression of the change in the surface potential for the sensor modified with the nanofilter with PBA relative to the sensor without PBA. The values were calculated using the average change in the surface potential at 31.6 nM for individual experiments with different samples. The left bar indicates ΔV_{out} of 100% for serotonin hydrochloride (SE), NE, EP, or dopamine hydrochloride (DA), which was obtained using the nanofilter without PBS (note that the standard deviations at 100% were 27, 20, 14, and 6% for SE, NE, EP, and DA, respectively). n.s., not significant, $^{**}P < 0.05$ vs 100% change in the surface potential at 31.6 nM. The error bars indicate the standard deviation in percentage. The number of experiments is the same as the numbers in Figure 2. (B) Performance of the sensor modified with the nanofilter with PBA to serotonin against norepinephrine, epinephrine, and dopamine. Percentage of ΔV_{out} represents the sensor response to catecholamines at 10 nM relative to the response to serotonin at 100 nM. The values were calculated using the average change in the surface potential (number of experiments shown in Figure 2) for individual experiments with different samples. $^{***}P < 0.005$ vs 100% (ΔV_{out} serotonin at 100 nM /ΔV_{out} serotonin at 100 nM). The number of experiments is the same as the numbers in Figure 2.

that of the nanofilter-modified substrate, indicating that both substrates have the same electrochemical activity, which enabled a successful comparison in the FET real-time measurement.

The changes in the surface potentials of the nanofilter-modified (nanofilter with PBA) and control (nanofilter without PBA) sensors were monitored in real-time while varying the concentration of the analytes in undiluted PBS. Figure 2 shows the changes in the surface potential of the nanofilter-modified (diamonds) and control (circle) sensors plotted against the concentrations of serotonin, norepinephrine, epinephrine, dopamine, and cortisol on a logarithmic scale. As shown in Figure 2A, the nanofilter-modified sensor showed a linear response to serotonin in the range of concentrations in blood (0.6–2 μM),[33] having a sensitivity of 23 mV/decade. Therefore, the sensor can quantitatively determine serotonin under physiological conditions without any dilution. The surface potential rapidly decreased upon the addition of

https://dx.doi.org/10.1021/acsami.9b19309
ACS Appl. Mater. Interfaces 2020, 12, 14761−14769

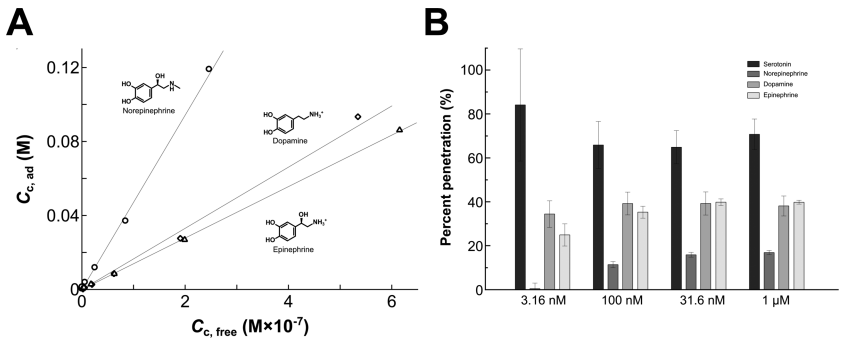

Figure 4. (A) Adhesion isotherm analysis of the response of the nanofilter-modified sensor to added catecholamines. (B) Relative amounts of serotonin and catecholamines that reached the Au electrode after passing through the nanofilter with PBA against those that reached the Au electrode after passing through the aryl-derivative multilayer without PBA at various concentrations. These results indicate the ratio of $C_{c,free}$ to C_c $[(C_{c,free}/C_c) \times 100\%]$, which is defined in the Supporting Information (see the section Isotherm analysis of the sensor response, in the Supporting Information p. S9). Also, this rate was calculated as the ratio of $\Delta V_{out}^{with\ PBA}$ obtained using the FET sensor with PBA to $\Delta V_{out}^{without\ PBA}$ obtained using the FET sensor without PBA $(\Delta V_{out}^{with\ PBA}/\Delta V_{out}^{without\ PBA}) \times 100\%$, from the data obtained in Figure 2.

serotonin to the solution and stabilized within 5 min (see Figure S5 in the Supporting Information). The sensitive detection was realized by the free penetration of serotonin through the nanofilter to approach the Au surface, where the direct surface electrochemical reaction on the highly active Au surface generated the change in the surface potential. As expected from the nanofilter design, the response of the control sensor (i.e., the sensor without PBA) had an almost negligible effect on the sensor response to serotonin, having a slightly higher sensitivity of 26 mV/decade. The detection sensitivity slightly decreased upon adding PBA to the nanofilter, probably because the addition of PBA partially filled the spaces in the multilayer film, which inhibited the penetration.

In contrast to the sensor response to serotonin, the inclusion or noninclusion of PBA in the nanofilter significantly affected the response to the interfering biomolecules, namely, norepinephrine, dopamine, and epinephrine (Figure 2B–D, respectively), or catecholamines as a group. The nanofilter-modified sensor with PBA significantly suppressed the changes in the surface potential, where the detection curve of the senor with PBA (Figure 2B–D, diamonds) shifted to the high concentration range compared with that of the sensor without PBA (Figure 2B–D, circles). The suppression occurred because catecholamines, having been captured by the nanofilter via the formation of stable esters between PBA and catecholamines, were prevented from approaching the Au sensing surface. Therefore, the nanofilter interface successfully distinguished the difference in the chemical structure between serotonin and catecholamines. Figure 2E shows the detection sensitivity of the sensor to the added cortisol. The addition of cortisol induced a negligible change in the Au surface potential, because cortisol is electrochemically inactive and did not react with the Au electrode.

Figure 3 shows the filtering effect of the nanofilter-modified EG-Au-FET biosensor obtained on the basis of the data shown in Figure 2. Figure 3A shows the suppression ratio of the nanofilter-modified sensor compared with the control sensor. The suppression ratio was calculated using the change in the surface potential at 31.6 nM of each analyte to clarify the effect of the nanofilter. The degree of suppression was as high as 70% for the detection of dopamine and epinephrine and reached 99.5% for norepinephrine. As discussed later, the degree of suppression depended on the boronate affinity.[34,35] Therefore, the nanofilter-modified sensor can specifically suppress the electrical signal from the interfering biomolecules having a catechol group. Figure 3B shows the performance of the sensor to the detection of serotonin. Here, the performance was calculated as the ratio of the electrical signal at a serotonin concentration of 100 nM to that at a catecholamine concentration of 10 nM, considering that the concentration of serotonin in blood is at least 2 orders of magnitude higher than that of catecholamines (0.6–2 μM for serotonin and 0–4 nM for catecholamines).[33] Figure 3B clearly shows that the nanofilter-modified sensor (with PBA) discriminated the electrical signal of serotonin from those of catecholamines in the detection range of serotonin in the blood. Moreover, the effect of the nanofilter with PBA on the electrical signal at each concentration was analyzed using the data shown in Figure 2, focusing on the electrical signals upon the addition of serotonin and norepinephrine (see Figure S6 in the Supporting Information). The gray bar shows the ratio of ΔV_{out} for norepinephrine detected using the control sensor without PBA to ΔV_{out} for serotonin detected using the nanofilter-modified sensor with PBA $(\Delta V_{NE,control}/\Delta V_{SE,nanofilter})$ and the black bar shows the ratio of ΔV_{out} for norepinephrine detected using the nanofilter-modified sensor with PBA to ΔV_{out} for serotonin detected using the nanofilter-coated sensor with PBA $(\Delta V_{NE,nanofilter}/\Delta V_{SE,nanofilter})$. Figure S6 shows that the latter ratio was sufficiently lower than the former ratio in a wide range of concentrations from 10 nM to 10 μM, although the difference between these ratios was not significant at above 10 μM for both serotonin and norepinephrine. Thus, the nanofilter with PBA clearly contributed to the increase in the S/N ratio for the detection of serotonin using the FET sensors. In addition, from the latter ratio, the electrical signal upon the addition of serotonin became higher than that upon the addition of norepinephrine at lower concentrations (<1 μM) detected using the nanofilter-modified sensor. The S/N ratio of serotonin signals with respect to dopamine and epinephrine signals may be improved by controlling the binding constant of the receptor in the nanofilter, as explained below.

Quantifying the effect of the nanofilter allows us to understand the mechanism of the specific suppression and gives a strategic insight to improve the sensor response. In this regard, the sensor response was characterized by adhesion isotherm analysis. We conducted the analysis by considering the covalent catecholamine/PBA binding as the adhesion of

https://dx.doi.org/10.1021/acsami.9b19309
ACS Appl. Mater. Interfaces 2020, 12, 14761–14769

the catecholamine to the specific binding site (PBA) in the nanofilter. Figure 4A shows the relationship between the concentrations of the unbound, free species ($C_{c,free}$) and the bound species ($C_{c,ad}$) at equilibrium (the detailed derivation of the equations are explained in the Supporting Information). The relationship between $C_{c,free}$ and $C_{c,ad}$ followed Henry's law because the analyte concentration is much lower than the buffer ion concentration. The linear slope represents the binding constant K_d; in this case, the binding constant of the adhesion of catecholamine to the nanofilter. The values of $\log K_d$ were 4.9, 4.4, and 4.3 for norepinephrine, dopamine, and epinephrine, respectively. Notably, the binding constants of norepinephrine/PBA and dopamine/PBA esters determined in the previous study were 4.81 and 4.56, respectively, which are comparable to those determined by adhesion isotherm analysis in this study.[36] The similarity between these values indicates that the quantitative effect of the suppression using the nanofilter interface directly reflects the binding capability of the receptor included in the nanofilter. Therefore, the performance of the sensor can be improved using receptors having higher binding constants for the interfering biomolecules. Moreover, the sensor response can be tuned to the appropriate concentration range of the analyte in bodily fluids by merely modifying the binding constant of the receptor in the nanofilter, which shows the potential of this strategy for various biosensing applications.

The relative amounts of serotonin and catecholamines reaching the Au electrode were estimated from the data shown in Figures 2 and 4A. Figure 4B shows the relative amounts of serotonin and catecholamines that reached the Au electrode after passing through the nanofilter with PBA against those that reached the Au electrode after passing through the aryl-derivative multilayer without PBA, that is, the filtering effect of the nanofilter with PBA at various concentrations. These results indicate the ratio of $C_{c,free}$ to C_c $[(C_{c,free}/C_c) \times 100\%]$, which is defined in the Supporting Information. Also, this rate was calculated as the ratio of $\Delta V_{out}^{\text{with PBA}}$ obtained using the FET sensor with PBA to $\Delta V_{out}^{\text{without PBA}}$ obtained using the FET sensor without PBA $(\Delta V_{out}^{\text{with PBA}}/\Delta V_{out}^{\text{without PBA}}) \times 100\%$. ΔV_{out} was generated by the oxidation reaction of small biomolecules reaching the Au electrode. As a result, the rate of each biomolecule did not change largely with respect to the change in the concentrations of serotonin and catecholamines, although the absolute value of ΔV_{out} increased with their increasing concentrations. In particular, regarding the relative amounts of norepinephrine that reached the Au electrode, the interaction of norepinephrine with the Au electrode was suppressed most effectively by the nanofilter with PBA, whereas serotonin more easily reached the Au electrode than catecholamines regardless of the presence of PBA. However, the relative amount of serotonin decreased to approximately 70% with the increasing serotonin concentration. This means that serotonin did not bind to PBA but encountered steric hindrance from the relatively densely packed aryldiazonium multilayer with PBA molecules. In fact, the charge transfer resistance (R_{CT}) of the aryldiazonium multilayer without PBA was increased by introducing PBA, as shown in Figure S7 and Table S1 (see the Supporting Information). That is, the electron transfer induced by the redox reaction of the ferricyanide/ferrocyanide mediator with the Au electrode may have been prevented by PBA molecules bound at the aryldiazonium multilayer.

Finally, we demonstrate the quantitative detection of serotonin with a high S/N ratio using the EG-Au-FET biosensor with the PBA–nanofilter interface in a model sample solution containing various stress biomarker interferences. Figure 5 shows the normalized responses of the sensors

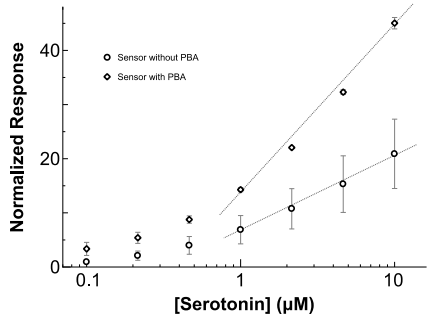

Figure 5. Normalized response of the sensor with (diamonds) and without (circles) PBA vs the serotonin concentration in a model sample solution containing 7.1 nM norepinephrine, 0.48 nM dopamine, 3.1 nM epinephrine, 1.7 μM cortisol, and 0.1 mg/mL HSA. Data were normalized by the following equation: $\Delta V_{norm} = (\Delta V_{out} - \Delta V_{blank})/\Delta V_{blank}$. Error bars represent the standard error of the two distinct experiments.

with PBA (diamonds) and without PBA (circles) to serotonin around the concentration range in blood in undiluted PBS containing 7.1 nM norepinephrine, 0.48 nM dopamine, 3.1 nM epinephrine, 1.7 μM cortisol, and 0.1 mg/mL HSA. The concentrations of dopamine, norepinephrine, epinephrine, and cortisol were twice the maximum concentrations in blood.[33] The nanofilter-modified sensor successfully and quantitatively determined serotonin even in the model sample solution containing interfering biomolecules with the sensitivity (slope) of 31 per decade. On the other hand, in the case of the sensor without PBA, the detection sensitivity to serotonin was 14, which was significantly lower than that of the PBA-included sensor. The sensitivity decreased because the interfering biomolecules could freely access the Au electrode by penetrating through the nanofilter without PBA, which led to competitive reactions on the Au sensing surface. The addition of the solution containing only the interfering biomolecules to the sensor, in fact, gave signals of 0.7 and 2 mV for the sensors with and without PBA, respectively. The slopes based on the normalization $[\Delta V_{norm} = (\Delta V_{out} - \Delta V_{blank})/\Delta V_{blank}]$ in Figure 5 show the effect of the blank signals (0.7 and 2 mV) for the sensors with and without PBA. That is, ΔV_{blank} = 0.7 for the sensor with PBA was lower than ΔV_{blank} = 2 for the sensor without PBA. Therefore, the quantitative determination of serotonin with the high S/N ratio in the model sample solution was realized using the EG-Au-FET biosensor with the sensing surface modified by the nanofilter interface with PBA as a receptor.

CONCLUSIONS

We proposed to enhance a S/N ratio for detecting a small-biomolecule stress marker, serotonin, using an EG-Au-FET biosensor with the surface functionalized by the nanofilter. The highly electromotive Au surface enabled highly sensitive recognition but without specificity or selectivity to the target biomolecule, serotonin. In this regard, we designed a nanofilter on a Au surface with a porous multilayer film with PBA so that only targeted small biomolecules, such as serotonin, but not

https://dx.doi.org/10.1021/acsami.9b19309
ACS Appl. Mater. Interfaces 2020, 12, 14761–14769

macrobiomolecules such as proteins, can come in contact with the Au surface through the multilayer film. Simultaneously, the PBA in the nanofilter captured small interfering biomolecules such as catecholamines before they reached the Au surface. As a result, the nonspecific electrical signal from the large biomolecules was specifically suppressed by 80% after the functionalization of the Au surface. Furthermore, the nanofilter-modified sensor could quantitatively detect serotonin in the range of serotonin concentrations in the blood with a sensitivity of 23 mV/decade. The sensor with PBA specifically suppressed the signal of catecholamine responses by up to 99.5%. Adhesion isotherm analysis revealed that the effect of the nanofilter directly reflected the binding constant of the interfering biomolecules and receptors. Therefore, one can improve or modulate the sensor response to the desired value by merely replacing the receptor in the nanofilter with one having sufficient affinity. Finally, we demonstrated the detection of serotonin with the high S/N ratio in a model of a bodily fluid containing norepinephrine, dopamine, epinephrine, cortisol, and HSA as interfering molecules. The sensor with PBA showed a quantitative response to serotonin with sufficiently high sensitivity, showing the possibility of the nanofilter design for various biosensing applications. In the future, we can improve the sensor stability by functionalizing the nanofilter surface with antifouling polymers. In this study, the nanoporous filter suppressed the nonspecific electrical signal of large biomolecules but large biomolecules may still adhere to the nanofilter surface, causing severe fouling of the surface. Therefore, in the future, the design and development of the polymeric nanofilter will be modified to improve the sensor response.

METHODS

Materials. Chemicals were used as received unless otherwise stated. Tetrabutylammonium hexafluorophosphate (nBu$_4$PF$_6$, 95%), 4-carboxy-3-fluorophenylboronic acid (FPBA), 4-(4,6-dimethoxy-1,3,5-triazine-2-yl)-4-methylmorpholinium chloride n-hydrate (DMT-MM, 98%), dopamine hydrochloride (DA), hydrocortisone (cortisol, 97%), albumin from human serum (HSA, 96%), albumin from bovine serum (BSA, 98%), α-amylase (AMY), potassium chloride (KCl), acetonitrile, acetone, methanol, ethanol, 1 M hydrochloric acid (HCl), and phosphate-buffered saline (PBS, 1×) were purchased from FUJIFILM Wako Pure Chemical Corporation. 4-Nitrobenzenediazonium tetrafluoroborate (NBD, 98%), serotonin hydrochloride (SE, 97%), L-noradrenaline bitartrate (norepinephrine, NE, 98%), L-adrenaline bitartrate (epinephrine, EP, 98%), and L-ascorbic acid (99%) were purchased from Tokyo Chemical Industry Co., Ltd.

Preparation of the PBA-Included Nanofilter-Modified Au Electrode. Au/Cr (100/10 nm) thin film sputtered on a glass substrate (7.5 cm × 2.5 cm) was purchased from Kyowa International. The substrates were cut into eight pieces with the same dimensions. Any organic contaminants were removed from the Au surface prior to the electrochemical grafting by immersing into acetone and methanol each for 10 min. Then, the cleaned Au electrode was pretreated with cyclic voltammetry (CV) in 100 mM nBu$_4$PF$_6$ in acetonitrile from 0.6 to 0.1 V vs Ag/AgCl for 2 cycles, in which the Au surface was electrochemically cleaned and activated. An electrochemical analyzer (618E, BAS Instruments) was used for the electrochemical surface treatments, and potential was applied through the Ag/AgCl reference electrode in the saturated KCl, which was connected to the acetonitrile solution through the salt bridge (agarose gel with 3 M KCl). Then, the cleaned Au electrode was immersed in acetonitrile solution (2 mM NBD and 100 mM nBu$_4$PF$_6$) in an ice bath, and potential was applied from 0.6 to 0.1 V vs Ag/AgCl for 3 cycles where the nitrobenzene (Ph-NO$_2$) multilayer was grafted on the Au electrode. The Ph-NO$_2$-grafted Au electrode was washed with methanol and distilled water and then dried in a flow of N$_2$.

In the next step, Ph-NO$_2$ was reduced to Ph-NH$_2$ by the following procedure. The Ph-NO$_2$-grafted Au electrode was immersed in a 10% ethanol solution containing 100 mM KCl, and potential was applied from 0 to −1.05 V vs Ag/AgCl for 10 cycles until the oxidative peak (peak II in Figure S1B) disappeared. The reduced samples were washed with distilled water and then dried in N$_2$ flow. PBA was introduced into the nanofilter layer by immersing the Ph-NH$_2$ modified Au electrode in a solution of 100 mM FPBA and 100 mM DMT-MM in methanol for 18 h. The control group was prepared in the same manner but in a different order. That is, the Ph-NO$_2$-grafted Au electrode was immersed in methanol containing FPBA (100 mM) and DMT-MM (100 mM) for 18 h before reducing the nitrophenyl group to the aminophenyl group via cyclic voltammetry.

Characterization of the Nanofilter-Modified Au Electrode Surfaces. The surface of the Au electrode was characterized by atomic force microscopy (AFM, Agilent 5500, Toyo Corporation). In the AFM measurement, images were collected by an AC tapping mode with the PPR-NCHR-10 probe (NANOSENSORS). For the characterization of surface morphology, the images were collected by measuring the surface roughness of the multilayer-coated Au electrode. For determining the multilayer thickness, only a part of the Au electrode was modified by the multilayer film by covering the Au surface with a photoresist. The photoresist was patterned on the Au electrode by photolithography, as briefly described in the following. The cleaned Au electrode (immersed in acetone and methanol for 10 min) was coated with a positive photoresist by spin coating (500 rpm for 5 s, followed by 3000 rpm for 30 s). After the prebaking process (110 °C for 3 min on a hot plate), the substrates were exposed to the ultraviolet (UV) light through a Cr-patterned glass mask for 4 s using a mask aligner (Q-2001CT, Quintel). The substrates were developed in a developer (NMD-W, 90 s), followed by the post-baking (120 °C for 3 min) on the hot plate. The photoresist-patterned substrates were coated by the multilayer film via cyclic voltammetry in a 2 mM NBD aqueous solution in 0.1 M HCl (0.5−0 V vs Ag/AgCl). The multilayer-grafted substrates were immersed in methanol for 12 h for lift-off. Finally, the AFM images were collected by measuring the gap between the unmodified/multilayer-grafted Au surfaces.

FET Real-Time Measurement. The potentiometric real-time measurement of the analytes was operated using a FET real-time monitoring system (Optogenesys). The nanofilter-modified Au electrodes were connected to the extended gate of the n-channel junction-type FET (K246-Y9A, Toshiba). The sensing surface was separated from the connection by the encapsulation with the polycarbonate ring (1 cm diameter). The sensing surface was covered with 500 μL 1× PBS buffer. In the measurement, a constant gate potential, V_G (2 V), was applied through the Ag/AgCl reference electrode, which was connected to the solution through the salt bridge (agarose gel with 3 M KCl). The drain voltage, V_D (5 V), was applied through the monitoring device to operate the device in a saturated region. The source−drain current, I_{DS}, was set to 700 μA, and the change in V_S was monitored by the source-follower circuit, which was extracted to the monitor as V_{out}. Therefore, in the operation system, change in V_{out} (ΔV_{out}) corresponds to the changes in the Au surface potential or the threshold voltage of the semiconductor (ΔV_T). After surface potential was stabilized, the analyte was added to the sensing solution to obtain the desired concentration. The analyte was added every 5 min, and the surface potential was taken as an average of five points (the sensor collects V_{out} every 0.5 s) in 280 s after changing the concentration. In the detection of serotonin, interfering biomolecules (dopamine, epinephrine, norepinephrine, cortisol, and HSA) were first added to the sensing solution to obtain a blank response.

https://dx.doi.org/10.1021/acsami.9b19309
ACS Appl. Mater. Interfaces 2020, 12, 14761−14769

■ ASSOCIATED CONTENT

Supporting Information

The Supporting Information is available free of charge at https://pubs.acs.org/doi/10.1021/acsami.9b19309.

Electrochemical grafting and reduction of the nitrobenzene multilayer film on the Au electrode (Figure S1); surface characterization of the multilayer-grafted film on the Au electrode using AFM (Figure S2); specific suppression of nonspecific electrical signals from large biomolecules using the multilayer-functionalized EG-Au-FET biosensor (Figure S3); reduction of the nitrophenyl multilayer before or after pre-treatment with PBA (Figure S4); real-time serotonin detection using a nanofilter-coated sensor (Figure S5); effect of a nanofilter with PBA on an electrical signal at each concentration (Figure S6); impedance analysis of the aryl-derivative multilayer with and without PBA (Figure S7); impedimetric parameters in the resistance−capacitance (RC) circuit of the modified Au electrodes (Table S1) (PDF)

■ AUTHOR INFORMATION

Corresponding Author

Toshiya Sakata − *Department of Materials Engineering, School of Engineering, The University of Tokyo, Tokyo 113-8656, Japan;* orcid.org/0000-0003-1246-5000; Phone: +81-3-5841-1842; Email: sakata@biofet.t.u-tokyo.ac.jp

Author

Shoichi Nishitani − *Department of Materials Engineering, School of Engineering, The University of Tokyo, Tokyo 113-8656, Japan*

Complete contact information is available at: https://pubs.acs.org/10.1021/acsami.9b19309

Notes

The authors declare no competing financial interest.

■ ACKNOWLEDGMENTS

This study was partly supported by the Mirai Program of Japan Science and Technology (JST). We would like to thank Professors M. Nakao and K. Nishi and Dr. M. Hagio of IoT Media Laboratory, the University of Tokyo, for their help and useful discussions.

■ REFERENCES

(1) Hammen, C. Stress and Depression. *Annu. Rev. Clin. Psychol.* **2005**, *1*, 293−319.

(2) Mazure, C. M. Life Stressors as Risk Factors in Depression. *Clin. Psychol. Sci. Pract.* **1998**, *5*, 291−313.

(3) Antoni, M. H.; Lutgendorf, S. K.; Cole, S. W.; Dhabhar, F. S.; Sephton, S. E.; McDonald, P. G.; Stefanek, M.; Sood, A. K. The Influence of Bio-Behavioural Factors on Tumour Biology: Pathways and Mechanisms. *Nat. Rev. Cancer* **2006**, *6*, 240−248.

(4) Pruessner, J. C.; Dedovic, K.; Pruessner, M.; Lord, C.; Buss, C.; Collins, L.; Dagher, A.; Lupien, S. J. Stress Regulation in the Central Nervous System: Evidence from Structural and Functional Neuroimaging Studies in Human Populations - 2008 Curt Richter Award Winner. *Psychoneuroendocrinology* **2010**, *35*, 179−191.

(5) Ritvanen, T.; Louhevaara, V.; Helin, P.; Väisänen, S.; Hänninen, O. Responses of the Autonomic Nervous System during Periods of Perceived High and Low Work Stress in Younger and Older Female Teachers. *Appl. Ergon.* **2006**, *37*, 311−318.

(6) Ulrich-Lai, Y. M.; Herman, J. P. Neural Regulation of Endocrine and Autonomic Stress Responses. *Nat. Rev. Neurosci.* **2009**, *10*, 397−409.

(7) Wu, K.; Fei, J.; Hu, S. Simultaneous Determination of Dopamine and Serotonin on a Glassy Carbon Electrode Coated with a Film of Carbon Nanotubes. *Anal. Biochem.* **2003**, *318*, 100−106.

(8) Cen, P.; Walther, C.; Finkel, K. W.; Amato, R. J. Biomarkers in Oncology and Nephrology. In *Renal Disease in Cancer Patients*; Elsevier, 2014; pp 21−38.

(9) Chaouloff, F.; Berton, O.; Mormède, P. Serotonin and Stress. *Neuropsychopharmacology* **1999**, *21*, 28−32.

(10) Yamakawa, K.; Matsunaga, M.; Isowa, T.; Ohira, H. Serotonin Transporter Gene Polymorphism Modulates Inflammatory Cytokine Responses during Acute Stress. *Sci. Rep.* **2015**, *5*, No. 13852.

(11) Kitade, T.; Kitamura, K.; Konishi, T.; Takegami, S.; Okuno, T.; Ishikawa, M.; Wakabayashi, M.; Nishikawa, K.; Muramatsu, Y. Potentiometric Immunosensor Using Artificial Antibody Based on Molecularly Imprinted Polymers. *Anal. Chem.* **2004**, *76*, 6802−6807.

(12) Swamy, B. E. K.; Venton, B. J. Carbon Nanotube-Modified Microelectrodes for Simultaneous Detection of Dopamine and Serotonin in Vivo. *Analyst* **2007**, *132*, 876.

(13) Clark, J. J.; Sandberg, S. G.; Wanat, M. J.; Gan, J. O.; Horne, E. A.; Hart, A. S.; Akers, C. A.; Parker, J. G.; Willuhn, I.; Martinez, V.; et al. Chronic Microsensors for Longitudinal, Subsecond Dopamine Detection in Behaving Animals. *Nat. Methods* **2010**, *7*, 126−129.

(14) Wang, P.; Xia, M.; Liang, O.; Sun, K.; Cipriano, A. F.; Schroeder, T.; Liu, H.; Xie, Y.-H. Label-Free SERS Selective Detection of Dopamine and Serotonin Using Graphene-Au Nanopyramid Heterostructure. *Anal. Chem.* **2015**, *87*, 10255−10261.

(15) Sharma, S.; Singh, N.; Tomar, V.; Chandra, R. A Review on Electrochemical Detection of Serotonin Based on Surface Modified Electrodes. *Biosens. Bioelectron.* **2018**, *107*, 76−93.

(16) Sakata, T. Biologically Coupled Gate Field-Effect Transistors Meet in Vitro Diagnostics. *ACS Omega* **2019**, *4*, 11852−11862.

(17) Kim, S. K.; Kim, D.; Jeon, S. Electrochemical Determination of Serotonin on Glassy Carbon Electrode Modified with Various Graphene Nanomaterials. *Sens. Actuators, B* **2012**, *174*, 285−291.

(18) Nishitani, S.; Sakata, T. Polymeric Nanofilter Biointerface for Potentiometric Small-Biomolecule Recognition. *ACS Appl. Mater. Interfaces* **2019**, *11*, 5561−5569.

(19) Bergveld, P. Development of an Ion-Sensitive Solid-State Device for Neurophysiological Measurements. *IEEE Trans. Biomed. Eng.* **1970**, *BME-17*, 70−71.

(20) Larisika, M.; Kotlowski, C.; Steininger, C.; Mastrogiacomo, R.; Pelosi, P.; Schütz, S.; Peteu, S. F.; Kleber, C.; Reiner-Rozman, C.; Nowak, C.; et al. Electronic Olfactory Sensor Based on A. mellifera Odorant-Binding Protein 14 on a Reduced Graphene Oxide Field-Effect Transistor. *Angew. Chem., Int. Ed.* **2015**, *54*, 13245−13248.

(21) Zope, B. N.; Hibbitts, D. D.; Neurock, M.; Davis, R. J. Reactivity of the Gold/Water Interface during Selective Oxidation Catalysis. *Science* **2010**, *330*, 74−78.

(22) King, D. E. Oxidation of Gold by Ultraviolet Light and Ozone at 25 °C. *J. Vac. Sci. Technol., A* **1995**, *13*, 1247−1253.

(23) Gooding, J. J. J. Advances in Interfacial Design for Electrochemical Biosensors and Sensors: Aryl Diazonium Salts for Modifying Carbon and Metal Electrodes. *Electroanalysis* **2008**, *20*, 573−582.

(24) Mahouche-Chergui, S.; Gam-Derouich, S.; Mangeney, C.; Chehimi, M. M. Aryl Diazonium Salts: A New Class of Coupling Agents for Bonding Polymers, Biomacromolecules and Nanoparticles to Surfaces. *Chem. Soc. Rev.* **2011**, *40*, 4143.

(25) Kong, B.; Zhu, A.; Luo, Y.; Tian, Y.; Yu, Y.; Shi, G. Sensitive and Selective Colorimetric Visualization of Cerebral Dopamine Based on Double Molecular Recognition. *Angew. Chem., Int. Ed.* **2011**, *50*, 1837−1840.

(26) Kajisa, T.; Li, W.; Michinobu, T.; Sakata, T. Well-Designed Dopamine-Imprinted Polymer Interface for Selective and Quantitative Dopamine Detection among Catecholamines Using a Potentiometric Biosensor. *Biosens. Bioelectron.* **2018**, *117*, 810−817.

(27) James, T. D.; Sandanayake, K. R. A. S.; Shinkai, S. Saccharide Sensing with Molecular Receptors Based on Boronic Acid. *Angew. Chem., Int. Ed.* **1996**, *35*, 1910−1922.
(28) Nishitani, S.; Sakata, T. Potentiometric Adsorption Isotherm Analysis of a Molecularly Imprinted Polymer Interface for Small-Biomolecule Recognition. *ACS Omega* **2018**, *3*, 5382−5389.
(29) Kajisa, T.; Sakata, T. Molecularly Imprinted Artificial Biointerface for Enzyme-Free Glucose Transistor. *ACS Appl. Mater. Interfaces* **2018**, *10*, 34983−34990.
(30) Himori, S.; Nishitani, S.; Sakata, T. Control of Potential Response to Small Biomolecules with Electrochemically Grafted Aryl-Based Monolayer in Field-Effect Transistor-Based Sensors. *Langmuir* **2019**, *35*, 3701−3709.
(31) Menanteau, T.; Levillain, E.; Downard, A. J.; Breton, T. Evidence of Monolayer Formation via Diazonium Grafting with a Radical Scavenger: Electrochemical, AFM and XPS Monitoring. *Phys. Chem. Chem. Phys.* **2015**, *17*, 13137−13142.
(32) Menanteau, T.; Dabos-Seignon, S.; Levillain, E.; Breton, T. Impact of the Diazonium Grafting Control on the Interfacial Reactivity: Monolayer versus Multilayer. *ChemElectroChem* **2017**, *4*, 278−282.
(33) Steckl, A. J.; Ray, P. Stress Biomarkers in Biological Fluids and Their Point-of-Use Detection. *ACS Sensors* **2018**, *3*, 2025−2044.
(34) Springsteen, G.; Wang, B. A Detailed Examination of Boronic Acid−Diol Complexation. *Tetrahedron* **2002**, *58*, 5291−5300.
(35) Bie, Z.; Chen, Y.; Ye, J.; Wang, S.; Liu, Z. Boronate-Affinity Glycan-Oriented Surface Imprinting: A New Strategy to Mimic Lectins for the Recognition of an Intact Glycoprotein and Its Characteristic Fragments. *Angew. Chem., Int. Ed.* **2015**, *54*, 10211−10215.
(36) Ptak, T.; Młynarz, P.; Dobosz, A.; Rydzewska, A.; Prokopowicz, M. Potentiometric and NMR Complexation Studies of Phenylboronic Acid PBA and Its Aminophosphonate Analog with Selected Catecholamines. *J. Mol. Struct.* **2013**, *1040*, 59−64.

https://dx.doi.org/10.1021/acsami.9b19309
ACS Appl. Mater. Interfaces 2020, 12, 14761−14769